

Analysis of the supra-thermal electrons during disruption instability in the T-10 tokamak

P.V.Savrukhin, A.V.Sushkov

Russian Research Center “Kurchatov Institute,” 123182, Moscow, Russia

Generation of electron beams with nonthermal energies ($E_\gamma \sim 100\text{keV}$) is one of the common feature of disruption instability in tokamaks [1,2]. Recent experiments in T-10 tokamak have indicated that the beams are often characterised by narrow localisation around magnetic surfaces with rational values of the safety factor ($q=1,2$). Such localisation of the beams can be connected with strong electric fields induced due to reconnection of the magnetic field lines during growth of the large-scale MHD perturbations (see [3]). Analysis [4] indicated, that while density of the nonthermal electrons induced during magnetic reconnection is two orders of magnitude smaller than the equilibrium plasma density, they can substitute considerable fraction of the plasma current around the rational q surfaces and can lead to growth of the runaway avalanches during major disruption. Present paper represents analysis of spatial localisation and temporal evolution of x-ray burst connected with the electron beams during density limit disruption and evaluate role of the primary electron beams in intensive hard x-ray spikes in post-disruptive plasma in the T-10 tokamak. The x-ray intensity is identified using standard Si detectors array and gas detectors with orthogonal view of the plasma column and in-vessel CdTe detectors with tangential view of the plasma column [5].

The x-ray bursts connected with the non-thermal electrons are observed most clearly in T-10 plasma, as well as in experiments in other tokamaks (see Ref. 1,2), during energy quench at the density limit disruption. Typical evolution of x-ray emissivity is shown in the case in Fig.1. Unstable plasma configuration with large-scale $m=1, n=1$ and $m=2, n=1$ modes is formed in the case after additional gas puffing at the quasi-stationary stage of the discharge ($t > 700\text{ms}$). Energy quench observed at $t=750.7\text{ms}$ (see Fig.1) is accompanied with intensive bursts of the x-ray emission. Energy quench leads to cooling down of the bulk plasma, increase of the total radiated power, and strong influx of impurities due to enhanced plasma-wall interaction. This follows by considerable increase of the loop voltage and production of beams of the runaway electrons, which eventually hit the plasma facing components (see “secondary” x-ray bursts at $t=756\text{ms}$ in Fig.1).

Relatively small size of the bright spots observed at the initial stage of the disruption (see $t=750.7\text{ms}$ in Fig.1) can indicate indirectly narrow localisation of the non-thermal electrons inside a specific area of the plasma cross section (see also [2]). The bright spots are typically observed when maximum x-ray perturbations (associated with position of the X-point of the $m=2$ magnetic island) are placed in field of view of the detectors. Appearance of the bursts at specific angular position of the MHD perturbations can indicate indirectly connection of the bursts with the $m=2$ magnetic island.

While typically observed at the initial stage of an energy quench, the x-ray bursts are also often observed prior to the disruption. The non-thermal x-ray bursts have maximum amplitude at the growing phase and at the top of the $m=2, n=1$ mode (see Fig.2). Amplitude of x-ray intensity during a single burst can be modulated in the case with repetition rate of order of 10-30 kHz (see [4]).

The burst are also observed in plasma after an energy quench at the density limit disruption. Time evolution of the plasma parameters is shown in the case in Fig. 3. Energy quench (appeared in the case in series of two minor disruptions at $t = 811.5\text{ ms}$ and $t = 824.0\text{ ms}$) is followed by intensive x-ray spikes observed with the TX array (see, *txray2* at $t > \sim 824\text{ ms}$ in Fig. 3). The spikes are generally observed as non-regular perturbation of the x-ray emissivity, while sometimes oscillations with typical repetition rates of order of $\gamma \sim 0.2\text{ ms}^{-1}$, 3 ms^{-1} , and $30 - 40\text{ ms}^{-1}$ can be identified in the signals (see Fig. 3). The repetition rate is close to one of the bursts observed prior the disruption in similar plasma conditions. The spikes represented in Fig. 3 are generally not observed with the orthogonal view x-ray array (*xcdtea2*) and gas detector (*xwda35*). This can indicate, indirectly, that spikes can appear as a result of forward bremsstrahlung radiation produced by nonthermal electrons “in flight” interacting with the residual plasma. Limited observation of the x-ray radiation during the “internal” spikes is in sharp contrast with hard x-ray bursts due to loss of the runaway electrons onto the vessel wall observed with all x-ray detectors.

Possible connection of the x-ray bursts with the electron beams accelerated in longitudinal equilibrium electric field can be checked in experiments with additional current ramp up just prior a disruption at high density (see Fig. 4). Growth of the plasma current is accompanied in the case by considerable increase of the longitudinal electric field at the outer part of the plasma. (Loop voltage is increased from quasi-stationary value $U_l \sim 1.5\text{ V}$ up to $U_l \sim 16\text{ V}$ just prior the energy quench and further up to $U_l \sim 70\text{ V}$ during disruption. It should be pointed out that power supply system used in T-10 for control of plasma current is capable to provide increase of the loop voltage even after the energy quench.) The process should be

accompanied by amplification of runaway electron beams with possible subsequent increase of the x-ray bursts amplitude. Growth of the x-ray intensity is in fact observed during secondary bursts after the energy quench in comparison with discharges with no current ramp-up [see $t > 822.6$ ms, in Fig. 4 and $t > 824$ ms in Fig. 3]. However, no considerable difference in amplitude of the x-ray perturbation prior the energy quench is observed in the experiments (see $t < 807.8$ ms in Fig. 4 and $t < 811.9$ ms in Fig. 3). While present experiments can not provide detailed information for qualitative comparison of the runaway electrons acceleration in both cases, it seems that increased loop voltage during current ramp-up (in the analysed U_l - range) does not change considerably initial stage of the disruption.

Further studies of the phenomena are planned in the T-10 tokamak using in-vessel array with adjustable field of view of the CdTe detectors.

The work is supported by Russian Fund for Basic Research (Grant 05-02-17294).

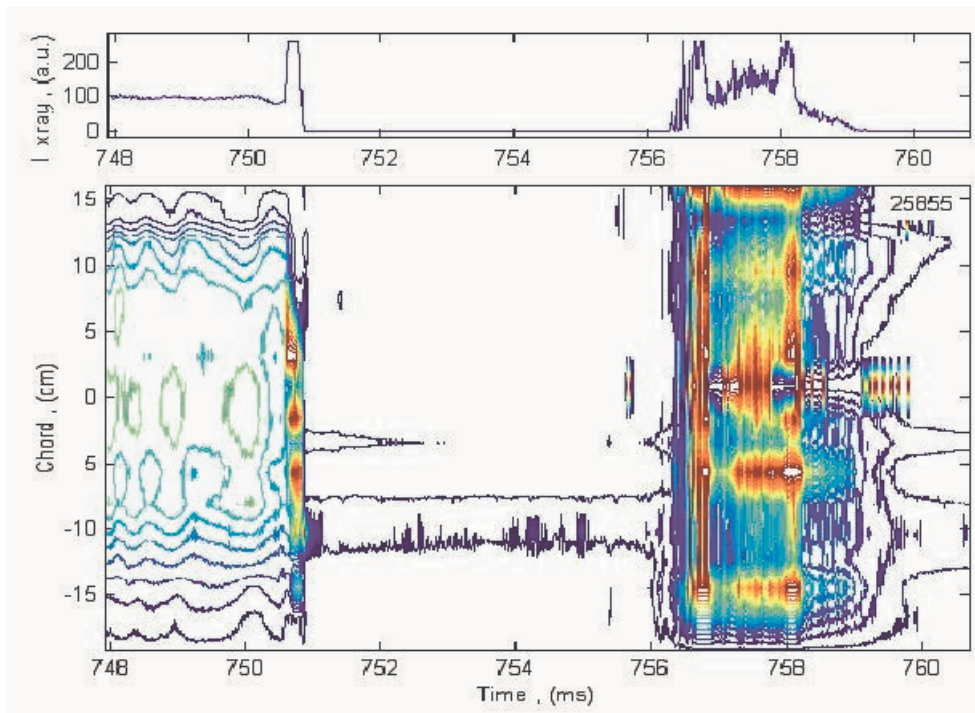


Fig.1. Time evolution of the x-ray intensity and x-ray contour plot measured during density limit disruption with the use of array of Si detectors with orthogonal view of the plasma column.

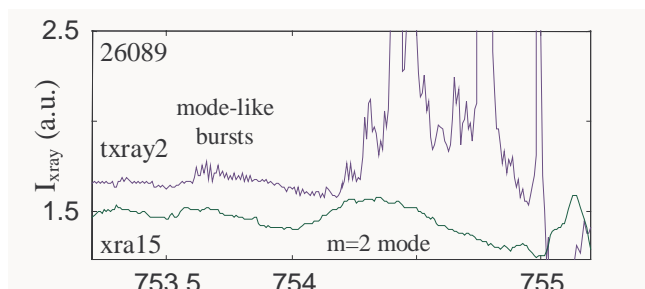


Fig.2. Time evolution of the x-ray intensity measured with the tangential (txray2) and orthogonal view (xra15) x-ray detectors just prior to the density limit disruption.

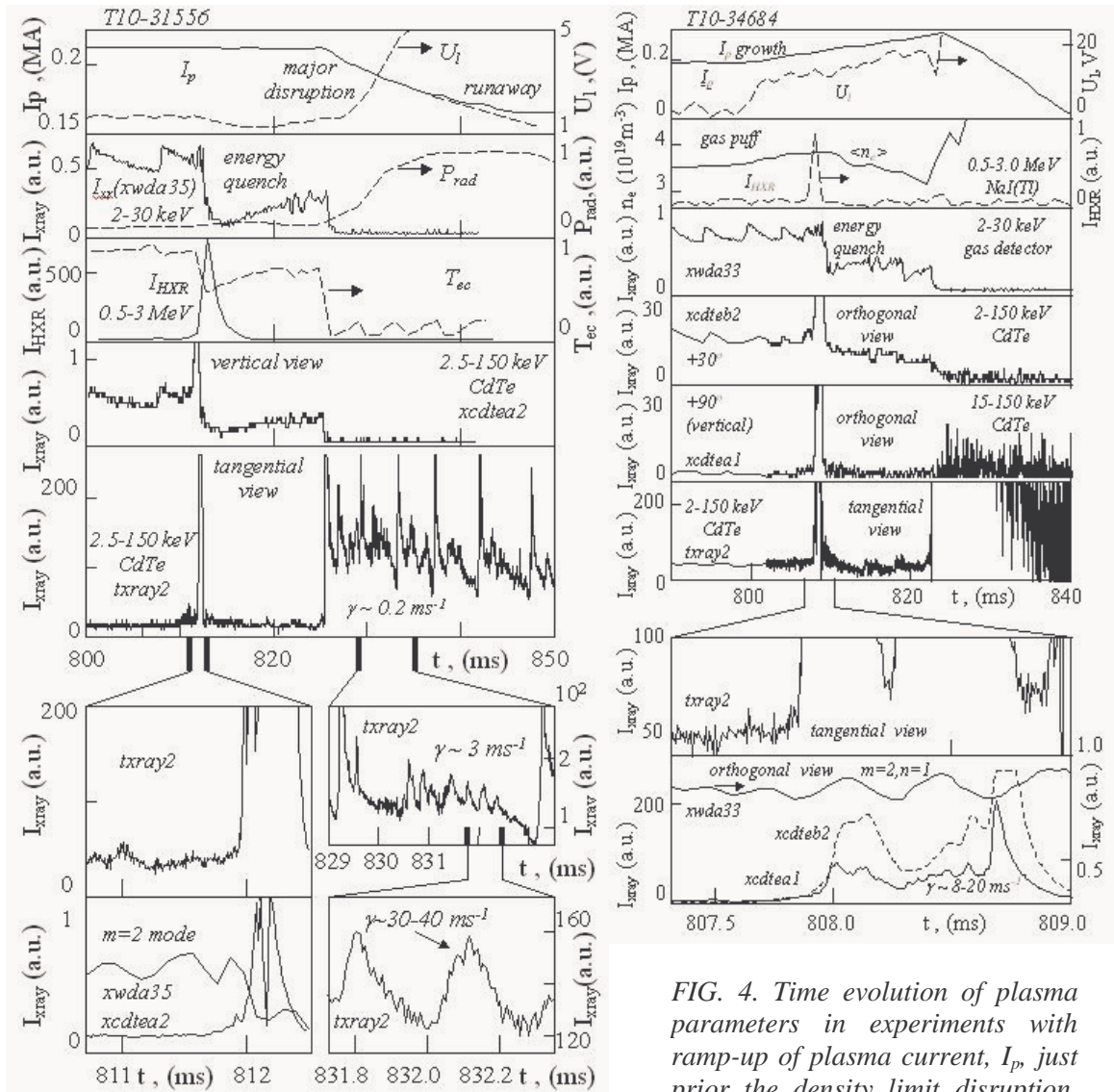


FIG. 3. Time evolution of plasma parameters after an energy quench during density limit disruption in ohmically heated plasma. Here, I_p is plasma current, U_1 loop voltage, P_{rad} total radiated power, T_{ec} electron (ECE) temperature, I_{HXR} hard x-ray intensity, $I_x(xwda35)$ x-ray intensity measured using XWDA gas detector. Also shown, intensity of the x-ray radiation measured using CdTe detectors with orthogonal ($xcdtea2$) and tangential ($txray2$) view of the plasma column.

FIG. 4. Time evolution of plasma parameters in experiments with ramp-up of plasma current, I_p , just prior the density limit disruption. Here, U_1 is loop voltage, $\langle n_e \rangle$ line averaged electron density, I_{HXR} hard x-ray intensity, $I_{xray}(xwda33)$ x-ray intensity measured using XWDA gas detector. Also shown, intensity of the x-ray radiation measured using CdTe detectors with orthogonal ($xcdtea1$, $xcdteb2$) and tangential ($txray2$) view of the plasma column.

- [1] ITER Physics Expert Group on Disruptions, Plasma Control, and MHD, ITER Physics Basis Editors, Nucl. Fusion **39**, 2251 (1999).
- [2] Gill, R. D., Alper, B., Edwards, A. W., *et al.*, Nucl. Fusion **40** (2000) 163.
- [3] Frank, A. G., Plasma Phys. Controlled Fusion **41** (1999) A687.
- [4] Savrukhin, P. V., Physics of Plasmas **9** (2002) 3421.
- [5] Savrukhin, P. V., Rev. Sci. Instrum. **73** (2002) 4243.